FEBS Letters 588 (2014) 584–593

FEBS Letters

journal homepage: www.FEBSLetters.org

Attenuation of hydrogen peroxide-mediated oxidative stress by *Brassica juncea* annexin-3 counteracts thiol-specific antioxidant (TSA1) deficiency in *Saccharomyces cerevisiae*

Ahan Dalal [a,*], Abhaypratap Vishwakarma [a], Naveen Kumar Singh [a], Triveni Gudla [a], Mrinal Kanti Bhattacharyya [b], Kollipara Padmasree [c], Andrea Viehhauser [d], Karl-Josef Dietz [d], Pulugurtha Bharadwaja Kirti [a]

[a] Department of Plant Sciences, School of Life Sciences, University of Hyderabad, Hyderabad, India
[b] Department of Biochemistry, School of Life Sciences, University of Hyderabad, Hyderabad, India
[c] Department of Biotechnology and Bioinformatics, School of Life Sciences, University of Hyderabad, Hyderabad, India
[d] Department of Plant Biochemistry and Physiology, Faculty of Biology, University of Bielefeld, Bielefeld, Germany

ARTICLE INFO

Article history:
Received 23 July 2013
Revised 15 December 2013
Accepted 2 January 2014
Available online 17 January 2014

Edited by Julian Schroeder

Keywords:
Brassica juncea annexin-3
Thioredoxin peroxidase 1
Oxidative stress
Complementation
Cross talk
Saccharomyces cerevisiae

ABSTRACT

***Brassica juncea* annexin-3 (BjAnn3) was functionally characterized for its ability to modulate H_2O_2-mediated oxidative stress in *Saccharomyces cerevisiae*. BjAnn3 showed a significant protective role in cellular-defense against oxidative stress and partially alleviated inhibition of mitochondrial respiration in presence of exogenously applied H_2O_2. Heterologous expression of BjAnn3 protected membranes from oxidative stress-mediated damage and positively regulated antioxidant gene expression for ROS detoxification. We conclude that, BjAnn3 partially counteracts the effects of thioredoxin peroxidase 1 (TSA1) deficiency and aids in cellular-protection across kingdoms. Despite partial compensation of TSA1 by BjAnn3 in cell-viability tests, the over-complementation in ROS-related features suggests the existence of both redundant (e.g. ROS detoxification) and distinct features (e.g. membrane protection versus proximity-based redox regulator) of both proteins.**

1. Introduction

Annexins represent ubiquitous proteins that are highly conserved among most eukaryotes. They comprise multigene family of calcium-dependent or -independent phospholipid-binding proteins [1–3]. For more than a decade, they are known to be transcriptionally regulated in response to various abiotic stressors and in dependence on diverse signaling pathways [3–18].

Arabidopsis thaliana annexin-1 (AtAnn1) was the first plant annexin protein that was functionally linked to oxidative stress response, and protected bacterial and mammalian cells from oxidative damage [4,19–21]. In line with this observation, *Brassica juncea* annexin-1 (BjAnn1), *Zea mays* annexins-33/35 (ZmAnn33/35), *Capsicum annuum* annexin-24 (CaAnn24), *Cynanchum komarovii* annexin (CkANN), *Gossypium hirsutum* annexin-1 (GhAnx1) and *Nelumbo nucifera* annexin-1 (NnANN1) proteins could also be associated with antioxidant function [10,13,14,22,23]. Initially, the conserved histidine residue of the first annexin repeat (His-40 in AtAnn1) was known to be associated with peroxidase activity [21,24]. Later, the concept was challenged, since peroxidase activity of plant annexin was proven to be independent of the heme-binding motif when ectopically expressed in plants or bacteria [12,22]. The published crystal structure of Anx(Gh1) from *G. hirsutum* (different from the *G. hirsutum* annexin mentioned above), suggested the putative triangular sulfur (S_3) cluster as redox-reactive center which functions in hydrogen peroxide (H_2O_2) reduction [25,26]. Presence of this cluster was later confirmed in AtAnn1 [12,27].

Our previous report demonstrated transcriptional up-regulation of *B. juncea* annexin-3 (*BjAnn3*) upon treatment with H_2O_2, sodium chloride, methyl viologen and wounding [11]. Based on this finding, we postulated that BjAnn3 is important for counteracting

Abbreviations: BjAnn3, *Brassica juncea* annexin-3; TSA1, thioredoxin peroxidase 1; ROS, reactive oxygen species; SOD1, superoxide dismutase 1; SOD2, superoxide dismutase 2; GPX2, glutathione peroxidase 2; TSA2, thioredoxin peroxidase 2

* Corresponding author. c/o Prof. P. B. Kirti, Department of Plant Sciences, School of Life Sciences, University of Hyderabad, Hyderabad 500046, India. Tel.: +91 9748781891.
E-mail address: ahan.dalal@daad-alumni.de (A. Dalal).

0014-5793/$36.00
http://dx.doi.org/10.1016/j.febslet.2014.01.006

sustained oxidative stress. Further, we proceeded with amino acid sequence analysis of BjAnn3 using ClustalW and Jalview [28,29], which revealed the absence of both heme-binding histidine residue and S_3 cluster (Supplemental Fig. 1). Cysteines are known to function as structural elements or redox switches [30]. They may contribute to multiple interactions of plant annexins with cytoskeleton, membranes and other proteins [31]. High cysteine (Cys) content in evolutionarily more ancient conifer annexins suggests their role in substitution for type 2 calcium-binding ligands in the loops for membrane interaction [31]. Cysteine rich annexin A10 from gastrointestinal mucous of human provides protection against microbes and fungi [32]. Cysteines play a crucial role as redox buffer in maintaining redox homeostasis for cell-survival on oxidative stress [30]. Two cysteine residues of BjAnn3 are highly conserved (Supplemental Fig. 1) among both plant and animal annexins [25], and might function in modulating or sensing oxidative stress [12,22]. The homology-modeled structure of BjAnn3 using SWISS-MODEL [33] and PyMOL (The PyMOL Molecular Graphics System, Version 1.4.1 Schrödinger, LLC.) showed that, the two conserved cysteine residues are positioned close to each other (Supplemental Fig. 2) and might contribute to disulfide bridge formation. Therefore, this study aimed at functional characterization of BjAnn3 following heterologous expression in *Saccharomyces cerevisiae*, in connection to H_2O_2-mediated oxidative stress response.

2. Materials and methods

2.1. Strains and culture conditions

Escherichia coli DH5α cells (Supplemental Table 1) were grown at 37 °C in Luria Bertani media. *S. cerevisiae* INVSc1 cells (Supplemental Table 1) were used for heterologous expression and assays. They were grown either in YPD medium (1% yeast extract, 2% peptone and 2% dextrose) or synthetic complete (SC) minimal medium (SC-ura) (0.67% yeast nitrogen base without amino acids, 2% glucose/raffinose as carbon source and dropout medium without uracil) at 30 °C. Protein expression was induced by adding 2% galactose as sole carbon source. In order to inactivate the *thioredoxin peroxidase 1* (*TSA1*) gene, *KANMX* cassette with *TSA1* flanking region was amplified using pFA6a-kanMX6 plasmid as template and the primer pair TSA1-KANMX-F/TSA1-KANMX-R. The PCR product was then transfected into INVSc1 cells for integration into *TSA1* and the cells were selected on G418 Sulfate (Calbiochem®, Germany)-containing YPD plates, to generate the *tsa1* null strain named as ADY1 (Supplemental Table 1). The knockout genotype was confirmed by gDNA PCR (genomic DNA isolated according to [34]) and RT-PCR (described below). *S. cerevisiae* ADY1 cells were used for complementation studies. Amplification primers for knockout generation and confirmation are listed in Supplemental Table 2.

2.2. Site-directed mutagenesis, cloning and recombinant plasmid construction

Standard molecular and biochemical methods were used for cloning of *BjAnn3* cDNA [35]. Total RNA isolated from *B. juncea* using TRI Reagent® (Sigma-Aldrich, USA), was used for first strand cDNA synthesis using oligo$(dT)_{23}$ primer (Sigma–Aldrich) and M-MLV Reverse Transcriptase (Sigma–Aldrich). *BjAnn3* cDNA was amplified using the primer pair BjAnn3-KpnI-F/BjAnn3-XhoI-R and Phusion High-Fidelity DNA Polymerase (Thermo Fisher Scientific Inc., USA). Cys_{114} and Cys_{242} were sequentially mutated to serine using primer pairs BjAnn3-C114S-F/BjAnn3-C114S-R and BjAnn3-C242S-F/BjAnn3-C242S-R, by site-directed mutagenesis as described by [36]. Both *BjAnn3* and $BjAnn3_{C114S/C242S}$ cDNAs were cloned into *KpnI* and *XhoI* sites of pYES2/NTA shuttle vector (Invitrogen™, USA) generating N-terminally His_6-tagged fragments. The correctness of the constructs was confirmed by sequencing (eurofins mwg|operon, Germany). Amplification primers for site-directed mutagenesis and cloning are listed in Supplemental Table 3.

2.3. Heterologous expression and immunodetection

INVSc1 and ADY1 cells transfected with empty and recombinant plasmids were selected on SC-ura + 2% glucose and maintained on SC-ura + 2% raffinose. For heterologous expression, 5 ml of liquid cultures in SC-ura + 2% galactose were grown overnight. The cultured-cells were sedimented and proteins were isolated using trichloroacetic acid (TCA) as described in [37,38]. The culture-pellets were washed once with sterile distilled water followed by 500 µl of 20% TCA. The pellets were then resuspended in 200 µl of 20% TCA and the suspensions were vortexed with glass beads at 4 °C for 30 min. The suspensions with lysed-cells were centrifuged (3000 rpm, 10 min at 25 °C) to collect the TCA-precipitated proteins and were further washed with 5% TCA. Each precipitate was dissolved in 60 µl of 1 × sample buffer [0.05 M Tris–HCl (pH 6.8), 2% sodium dodecyl sulfate (SDS), 10% glycerol and 0.1% bromophenol blue] supplemented with 6.66 µl of 1 M DTT and 33 µl of 1 M Tris–HCl (pH 9.0). The protein samples were boiled for 3–5 min; centrifuged (14000 rpm, 5 min at 25 °C) and finally the supernatants were loaded on 12% sodium dodecyl sulfate polyacrylamide gel electrophoresis (SDS–PAGE). The resolved proteins were then electroblotted onto polyvinylidene difluoride (PVDF) membrane and probed with mouse monoclonal Anti-polyHistidine antibody (Sigma–Aldrich) (dilution: 1:6000) followed by goat anti-Mouse IgG-ALP secondary antibody (Merck, Germany) (dilution: 1:3000). The blot was developed using BCIP/NBT (5-bromo-4-chloro-3-indolyl phosphate/nitro-blue-tetrazolium chloride) solution (Bangalore Genei, India).

2.4. Growth in liquid media and phenotypical analysis

Freshly grown cultures (OD_{600} = 0.7–1) after secondary inoculation in SC-ura media containing 2% galactose were diluted to OD_{600} = 0.2 with the same media. Oxidative stress was elicited with different concentrations of H_2O_2. After 12 h, cell density was estimated at OD_{600} and the percent ratio was calculated.

In addition, diluted culture of OD_{600} = 0.2 were treated with 2 and 2.5 mM H_2O_2 for 4 h and aliquots were spotted by serial dilution on YPD plates for phenotypic analysis. Viability was determined with fluctuation assay by plating 1000 cells based on OD_{600} (cell number in liquid culture was confirmed by plating for viable colonies under control conditions) from treated and untreated samples on YPD plates. Plates were photographed and colonies were counted after 48 h.

2.5. Oxygen consumption under oxidative stress

Exponentially grown cultures (OD_{600} = 0.7–1) after secondary inoculation in SC-ura liquid media containing 2% galactose, were sedimented, washed twice and finally re-suspended in fresh minimal media at a density of approximately 20 OD_{600} units. Cell-suspension (25 µl) was added into the oxygraph chamber to make up to a final reaction volume of 1 ml with minimal medium. The cell re-suspension procedure and the final cell number used in oxygraph chamber were optimized [39]. Respiratory oxygen consumption rates were monitored using a Clark-type oxygen electrode (Hansatech Instruments Ltd., England) for 10 min with and without H_2O_2.

2.6. Intracellular reactive oxygen species (ROS) production

Cells washed as before were re-suspended at a density of approximately 10 OD_{600} units. Cells were treated with H_2O_2 for 10 min and then incubated with 10 μM 2′,7′-dichlorofluorescein diacetate (DCFDA; Sigma–Aldrich) for 10 min in the dark at 25 °C. The cells were washed twice with the same media for removal of unincorporated dye and immediately imaged under a LSM 710 NLO ConfoCor 3 laser-scanning confocal fluorescence microscope (Carl Zeiss, Germany) at λ_{em} = 529 nm (λ_{exc} = 495 nm). OD of cells, H_2O_2 concentrations and time of treatment, time and temperature of DCFDA treatment were adjusted as appropriate [40]. 2′,7′-dichlorofluoresecin (DCF) fluorescence intensity was quantified in equal number of cells for each treatment from three different experiments using Image-J 1.42 software (NIH, USA).

2.7. Plasma membrane permeabilization

Cells re-suspended at a density of approximately 10 OD_{600} units were treated with H_2O_2 for 75 min, and subsequently incubated with 5 μg ml^{-1} propidium iodide (PI; Sigma–Aldrich) for 30 min in dark at 30 °C. The cells were washed twice and imaged under a LSM 710 NLO ConfoCor 3 laser-scanning confocal fluorescence microscope at λ_{em} = 620 nm (λ_{exc} = 530 nm) in order to check for viability and plasma membrane integrity. Intact plasma membrane is impermeable to PI. Upon loss of membrane integrity, PI penetrates the cell and intercalates in DNA. Thus PI is used as viability stain. Time and concentration of PI treatment was adjusted [41]. DNA-bound PI fluorescence intensity was quantified in equal number of cells for each treatment from three different experiments using Image-J 1.42 software (NIH, USA).

2.8. RNA isolation from S. cerevisiae, semi-quantitative RT-PCR and quantitative RT-PCR

Cultures diluted to an OD_{600} = 0.5 were treated with 2.5 mM H_2O_2 for 75 min. RNA was isolated from 10 ml of liquid cultures by acid phenol method as described in [38,42]. After short centrifugation, the pellet was resuspended in 400 μl of TES buffer [10 mM Tris–HCl (pH 7.5), 10 mM EDTA and 0.5% SDS] followed by addition of 400 μl of phenol (pre-equilibrated with DEPC-treated water). The mixture was incubated at 65 °C for 1 h, with intermittent vortexing. The mixture was rapidly chilled on ice for 5 min and centrifuged (14000 rpm, 10 min) at 4 °C. The aqueous layer was mixed with 400 μl of chloroform, vortex-mixed and centrifuged with same conditions as described above. RNA was precipitated from the extracted aqueous phase by addition of 1/10th volume of 3 M sodium acetate (pH 5.2) and 2.2 volume of pre-chilled ethanol. After centrifugation, the RNA pellet was washed with 70% ethanol and dissolved in 30 μl of DEPC-treated water. Equal amount of RNA was treated with DNase I (Sigma–Aldrich) according to manufacturer's protocol followed by cDNA synthesis using oligo$(dT)_{23}$ primer and M-MLV Reverse Transcriptase. cDNA samples were diluted appropriately and were subjected to semi-quantitative RT-PCR and qRT-PCR using gene-specific primers (Supplemental Table 4). SapphireAmp® Fast PCR Master Mix (Takara Bio Inc., Japan) was used for semi-quantitative RT-PCR. The reaction mixtures were pre-incubated for 1 min at 94 °C followed by 30 cycles of denaturation for 5 s at 98 °C, annealing for 5 s at 55 °C and extension for 5 s at 72 °C, in a Mastercycler® (Eppendorf, Germany). For qRT-PCR, FastStart Universal SYBR Green Master (Rox) (Roche Applied Science, Germany) was used. The reaction mixtures were pre-incubated at 95 °C for 10 min followed by 40 cycles of denaturation at 95 °C for 15 s, annealing at 59 °C for 30 s and extension at 72 °C for 30 s, in a Mastercycler® ep *realplex4* (Eppendorf). The relative gene-expression was analyzed using $2^{-\Delta\Delta Ct}$ method.

3. Results and discussion

The work aimed at understanding the role of BjAnn3 in H_2O_2-mediated oxidative stress. Externally applied H_2O_2 induces intracellular oxidative stress in yeast due to its water solubility and membrane permeability. Cells generate H_2O_2 both under basal and stressed growth conditions [43]. TSA1, the major 2-Cys peroxiredoxin in yeast, detoxifies hydroperoxides [44,45] and functions as a key regulator of intracellular ROS, especially H_2O_2, in *S. cerevisiae* [46]. *tsa1* null mutants are viable and indistinguishable from parental wild-type under aerobic control conditions, but display a remarkably H_2O_2-sensitive phenotype [40]. *TSA1* was knocked out in regular INVSc1 strain to generate the *tsa1* null mutant named as ADY1. Genomic DNA PCR (Fig. 1A) using primer pair KANMX-F/TSA1-R amplified a fragment connecting KANMX cassette and 3′ end of *TSA1* from ADY1 cells, with no amplification from INVSc1 cells. On the other hand, TSA1-F/TSA1-R primer pair resulted in gDNA PCR amplification from *TSA1* in INVSc1 cells, with no amplification from ADY1 cells. This result shows the absence of *TSA1* in ADY1 cells, which was further confirmed in transcript levels using TSA1-F/TSA1-R primer pair by semi-quantitative RT-PCR and qRT-PCR (Fig. 1B). Both strains were transfected either with empty vector pYES2/NTA or recombinant pYES2/NTA-*BjAnn3* clone to create four different strains, INVc, INV-ANNw, ADYc and ADY-ANNw. BjAnn3 expression was confirmed by Western blotting in INV-ANNw and ADY-ANNw cells (Fig. 1C).

To assess the role of BjAnn3 expression in oxidative stress, the four strains were treated with H_2O_2 in liquid culture (Fig. 1D). Heterologous expression of BjAnn3 increased growth rate of ADY1 cells by 18% in the absence of H_2O_2, but by 44% at 1 mM H_2O_2, and by more than 100% at 2 mM H_2O_2. These observations are in line with earlier findings [44,46]. Apparently, BjAnn3 efficiently counteracted the lost TSA1 function in ADY-ANNw cells (Fig. 1D). The data suggest a protective role of BjAnn3 in cellular-defense against oxidative stress. Based on the results, H_2O_2 concentrations of 2 and 2.5 mM were chosen for further experiments.

We hypothesized that, BjAnn3 might protect mitochondrial respiration during oxidative stress response (Fig. 1E). At 2 mM H_2O_2, respiration of cells overexpressing BjAnn3 showed no significant difference when compared with their respective wild-types. But at 2.5 mM H_2O_2, BjAnn3 overexpression stimulated respiratory activity of INVSc1 and ADY1 cells by 28% and 20%, respectively. Apparently, the presence of BjAnn3 partially mitigated oxidative stress-induced inhibition of mitochondrial respiration. ADYc cells had improved respiration compared to INVc cells upon treatment. TSA1 plays a prominent role in cellular-protection against hydroperoxide-mediated oxidative stress in respiratory-incompetent cells compared to wild-type. In addition, H_2O_2 treatment stimulates *TSA1* expression more in cells with dysfunctional mitochondria than in wild-type [44]. Based on the above studies, a possible explanation could be that, compromised TSA1 resulted in compensational elevation of respiration activity in order to maintain a balanced metabolism. Our results from Fig. 1E suggest that, BjAnn3 aids in cellular-protection against oxidative stress, thereby safeguards mitochondrial respiration.

In order to further substantiate our findings, we performed growth assays on plates (Fig. 2A). Viability of all four strains was indistinguishable under normal aerobic condition, while it varied in presence of H_2O_2. INV-ANNw cells appeared to be slightly more tolerant than INVc cells when treated with 2.5 mM H_2O_2, whereas no significant difference was seen at 2 mM H_2O_2. ADYc cells were more sensitive to H_2O_2 at both concentrations compared to INVc

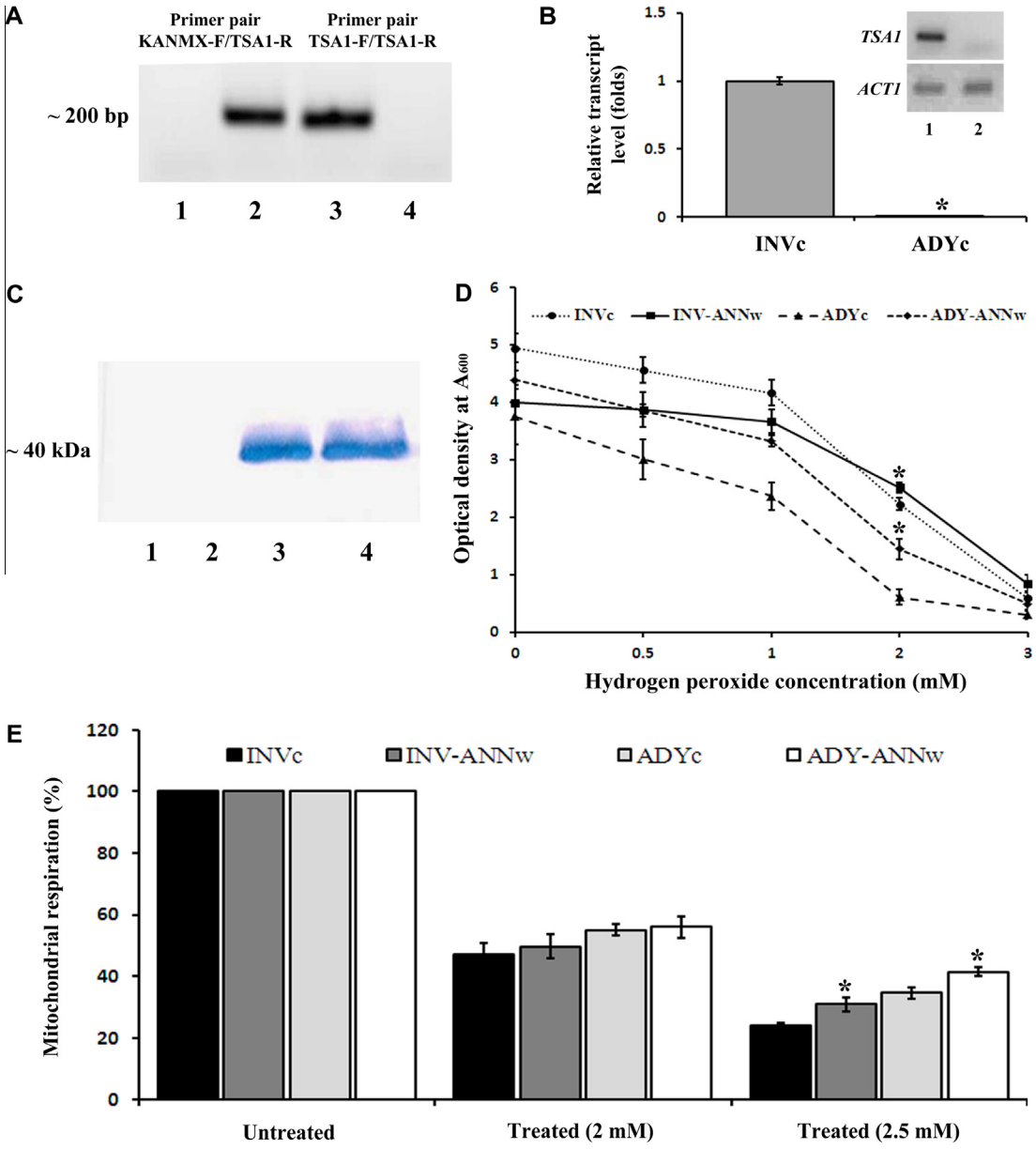

Fig. 1. PCR-based confirmation of *TSA1* knockout, recombinant expression of BjAnn3 in yeast and its functional effect on cell growth and respiration. (A) Confirmation of *TSA1* knockout by genomic DNA PCR in *lane1* and 3: INVc and *lane2* and *4*: ADYc cells. (B) Semi-quantitative RT-PCR (*Lane1*: INVc and *Lane2*: ADYc cells) and qRT-PCR analysis for verification of *tsa1* null mutant. *ACT1* was used as reference gene. (C) Confirmation of BjAnn3 expression in *lane1*, INVc; *2*, ADYc; *3*, INV-ANNw; *4*, ADY-ANNw cells. (D) Cell growth in presence of different concentrations of H_2O_2. (E) Mitochondrial respiration in percent of untreated cells. Data represent means ± S.D. from three measurements. Statistical analysis was carried out in SigmaPlot 11.0 by One-Way ANOVA (analysis of variance) with Duncan's Multiple Range Test (DMRT). (∗) marks significant differences with $p < 0.05$ relative to the likewise treated wild-type.

cells, which is consistent with earlier reports [44,46]. Expression of BjAnn3 restored cell-viability of ADYc cells close to the level of INVc cells. Cell-viability was quantified using fluctuation assay (Fig. 2B). Survival rate of INV-ANNw cells in 2 and 2.5 mM H_2O_2 increased by 14.7% and 16.5%, respectively, compared to the likewise treated wild-type. Viability of ADY-ANNw cells increased by 20.3% and 19.6% in 2 and 2.5 mM H_2O_2, respectively, when compared with treated wild-type. *TSA1* knockout resulted in 31.2% and 28.4% observed mortalities of ADYc cells in presence of 2 and 2.5 mM H_2O_2, respectively, which agrees with previous reports [44]. BjAnn3 expression in ADY1 cells partially complemented the loss of TSA1 function, indicating a significant protective role of BjAnn3 against H_2O_2-mediated oxidative stress.

Oxidative stress affects the structural integrity of phospholipids by lowering membrane lipid packing and facilitating phase separation [47,48]. One of the primary roles of annexins is seen in protecting cell membrane permeability by their highly conserved annexin core domain [49]. Plant annexins which respond to oxidative stress in a membrane-bound state, might bind or decompose peroxidated lipids, thereby restoring membrane stability and integrity. Alternatively, a protective mechanism of annexins on membranes may involve formation of two dimensional crystal patches on peroxidated membranes or fostering of membrane resealing [27]. Therefore, the next experiment investigated the capability of expressed BjAnn3 to maintain membrane integrity, which may be one of the underlying mechanisms to restore cell-viability upon oxidative stress. H_2O_2 treatment resulted in pronounced increase of cellular PI fluorescence in all four strains compared to their respective untreated controls, indicating an increase in plasma membrane permeability (Fig. 3A). Loss of *TSA1* in ADYc

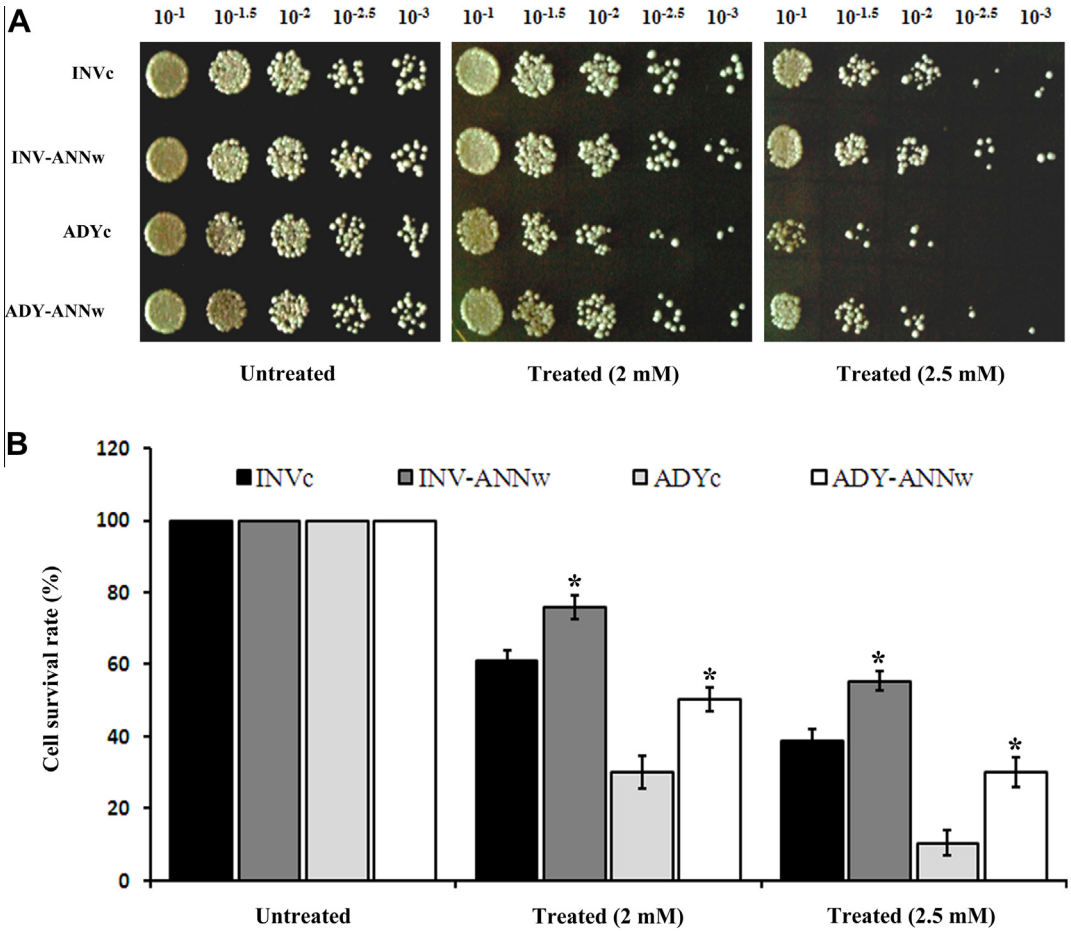

Fig. 2. Restoration of cell viability by BjAnn3 expression during H_2O_2-mediated oxidative stress. Sensitivity of yeast strains INVc, INV-ANNw, ADYc and ADY-ANNw to H_2O_2 was analyzed by spotting (A) and fluctuation assay with cell survival rate in percent of untreated cells (B). Data represent means ± S.D. from three measurements. Statistical analysis was carried out in SigmaPlot 11.0 by One-Way ANOVA with DMRT. (∗) marks significant differences with $p < 0.05$ relative to the likewise treated wild-type.

cells further enhanced PI fluorescence upon H_2O_2 treatment. BjAnn3 overexpression counteracted the PI fluorescence increase in INV-ANNw and ADY-ANNw cells. Quantification of PI fluorescence confirmed that, BjAnn3 strongly quenched the fluorescence in both INV-ANNw and ADY-ANNw cells (Fig. 3B). At both H_2O_2 concentrations, BjAnn3 was able to complement the loss of TSA1 function, with fluorescence quenched below the level as seen in INVc cells. These data support the conclusion that, annexins protect membranes against oxidative stress, which is in line with previous findings [27].

The role of plant annexins in improved ROS detoxification has been shown in both native [12] and transgenic plants [10,13,14,21,22,50,51]. ROS is formed due to normal yeast metabolism. Its release is enhanced in response to environmental stress [43]. In order to explore the possible link between BjAnn3 expression, increased cell-viability, plasma membrane protection and ROS formation, cells were subjected to DCFDA staining and analyzed by confocal microscopy (Fig. 4A). The DCF fluorescence level upon H_2O_2 treatment was highest in TSA1-deficient ADYc cells. Similar results were reported by Wong et al. [40]. BjAnn3 overexpression decreased the DCF fluorescence in H_2O_2-treated INV-ANNw and ADY-ANNw cells. When treated with 2 and 2.5 mM H_2O_2, BjAnn3 was able to suppress ROS accumulation by 20% and 35%, respectively in INV-ANNw cells, and by 23% and 38%, respectively in ADY-ANNw cells (Fig. 4B). ADYc cells generated 28.5% more ROS compared to INVc cells in presence of 2 mM H_2O_2, while no significant difference was observed upon 2.5 mM H_2O_2 treatment. This insignificant increase of ROS at higher H_2O_2 concentration may tentatively be explained by saturation of the stress effect. Overexpression of BjAnn3 compensated for the loss of TSA1 function as indicated by DCF fluorescence which was lower than that in INVc cells at 2 mM H_2O_2. The result is consistent with that from PI assay. Apparently, BjAnn3 lowers ROS accumulation and thus combats oxidative stress and increases cell-viability.

BjAnn3 has four cysteine residues, namely Cys_{114}, Cys_{129}, Cys_{226} and Cys_{242} (Supplemental Fig. 1). In their comprehensive review, Clark et al. [31] summarized the possible functions of highly conserved cysteine residues, in particular Cys_{111} (Cys_{114} in BjAnn3), and suggested that, it mediates redox sensitivity and interaction with external partners. In addition to disulfide bridge formation, redox regulation may also involve S-nitrosylation [52] or S-glutathionylation [12] of annexins. The redox switch likely interferes with the calcium-binding ability and calcium-dependent functions of annexins [31]. Based on protein modeling studies (Supplemental Fig. 2), Cys_{129} and Cys_{226} are predicted to be distantly positioned on the protein surface. On the other hand, Cys_{114} and Cys_{242} remained adjacent to each other (~5.3 Å) and might participate in disulfide bridge formation [53]. It may be proposed that, the two highly conserved cysteine residues (Cys_{114} and Cys_{242}) of BjAnn3 (Supplemental Fig. 1) might be responsible for ROS detoxification [12]. Therefore, we mutated these two cysteine residues of BjAnn3 to generate $BjAnn3_{C114S/C242S}$, and performed complementation assay (Fig. 5). Both INVSc1 and ADY1 cells were transfected with recombinant pYES2/NTA-*BjAnn3*$_{C114S/C242S}$ clone to create two different

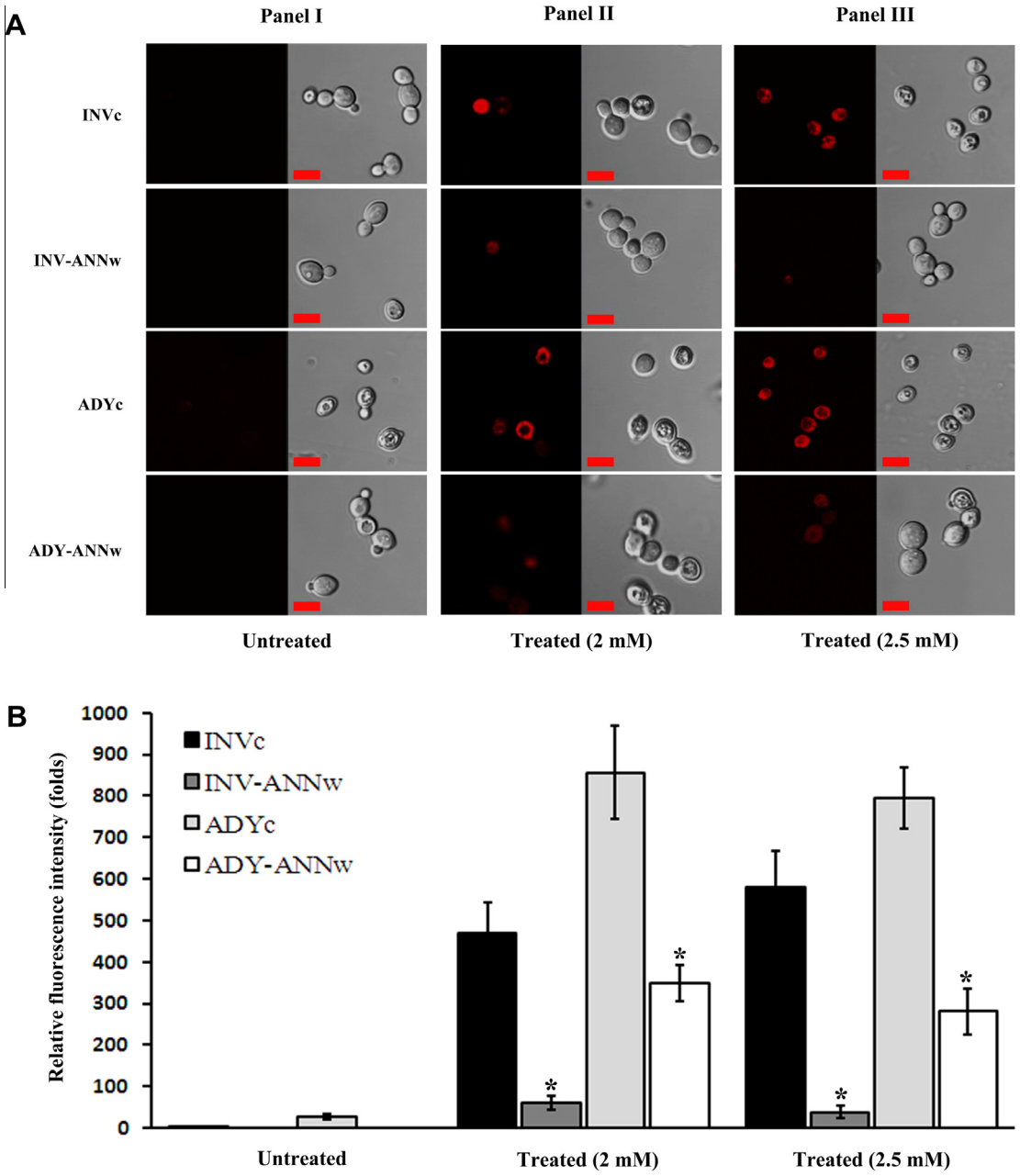

Fig. 3. Effect of BjAnn3 expression on membrane permeability upon H_2O_2-mediated oxidative stress. Propidium iodide (PI) fluorescence was observed under a confocal microscope; scale bars: 5 μm (A) and fluorescence intensity was quantified from more than 100 cells in each sample by using Image-J (B). Values are expressed as a fraction of the control (untreated INVc cells). Data represent means ± S.D. from three replicates. Data were analyzed for statistically significant differences using SigmaPlot 11.0 by One-Way ANOVA with DMRT. (*) marks significant differences with $p < 0.05$ relative to the likewise treated wild-type.

strains, INV-ANNv and ADY-ANNv. BjAnn3$_{C114S/C242S}$ expression was confirmed by Western blotting in INV-ANNv and ADY-ANNv cells (Fig. 5A). Growth assay on plates showed that, BjAnn3$_{C114S/C242S}$ expression could not protect INV-ANNv and ADY-ANNv cells efficiently upon H_2O_2 treatment when compared with their respective treated wild-types. The mutated protein failed to restore the lost cell-viability of ADYc cells upon treatment (Fig. 5B). Fluctuation assay clearly showed no significant protective role of the protein in INV-ANNv and ADY-ANNv cells upon H_2O_2 treatment when compared with their respective treated wild-types (Fig. 5C). Due to the absence of both heme-binding histidine residue and S_3 cluster in BjAnn3, the conserved cysteine residues are likely important components of the oxidative stress response. Since cysteine thiols participate in conformational stability [30], their mutation may result in conformational changes which could be studied by circular dichroism spectroscopy. The data indicate that, the loss of BjAnn3 function is a direct cause of cysteine mutation. Apparently, BjAnn3$_{C114S/C242S}$ expression could not counteract the loss of TSA1 function effectively in ADY1 cells, indicating a prominent role of the conserved cysteine residues in ROS detoxification.

In the next step, we investigated the effects of BjAnn3 expression which could indirectly affect cellular ROS levels. Earlier experiments have linked plant annexins to other genes involved in improved stress response [10,50,54]. To this end, transcript levels of *superoxide dismutase 1* (*SOD1*) (Fig. 6A), *superoxide dismutase 2* (*SOD2*) (Fig. 6B), *glutathione peroxidase 2* (*GPX2*) (Fig. 6C) and *thioredoxin peroxidase 2* (*TSA2*) (Fig. 6D) were quantified by qRT-PCR. The antioxidant genes were transcriptionally up-regulated in

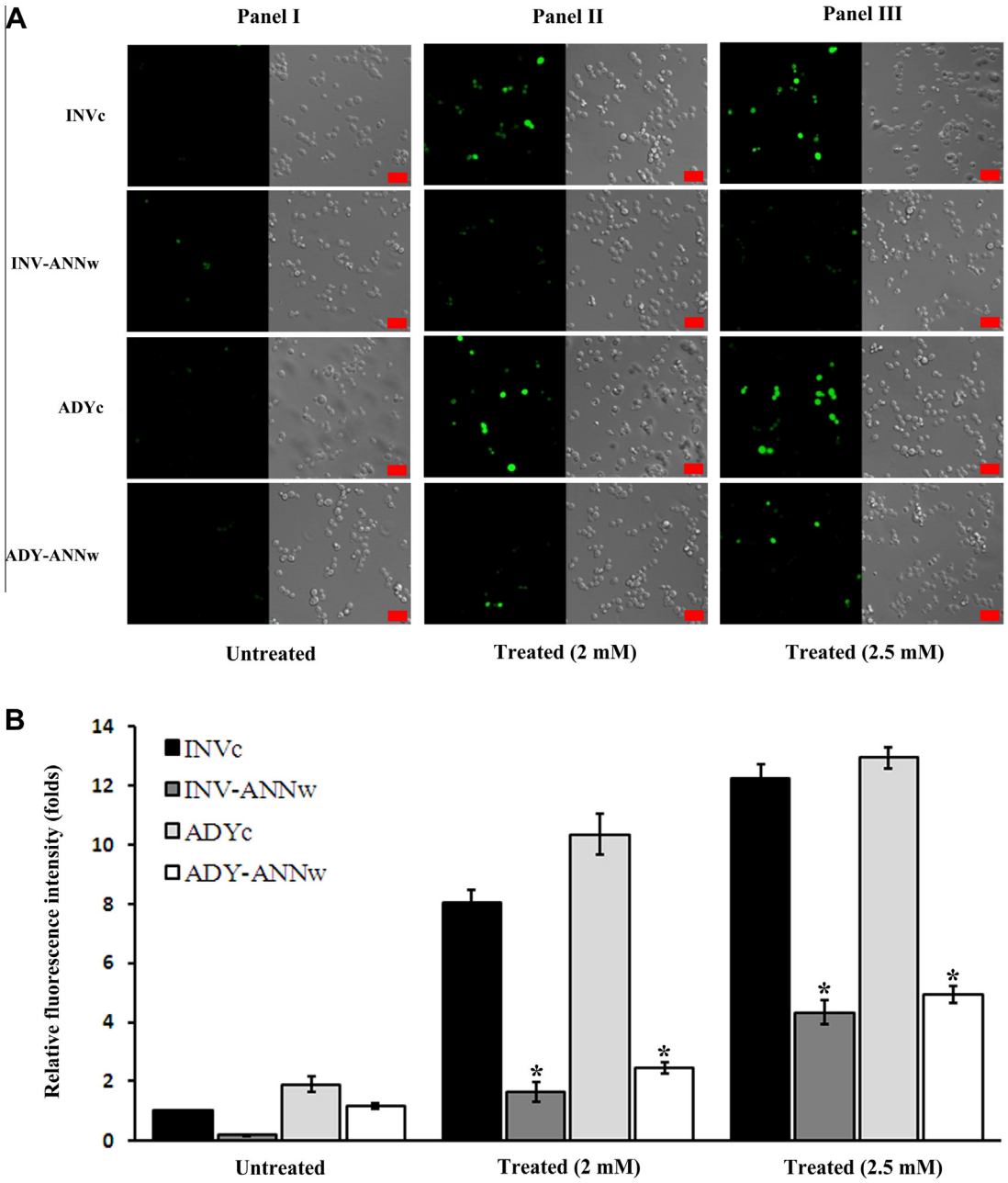

Fig. 4. Modulation of H_2O_2-mediated ROS accumulation by BjAnn3. ROS was detected by DCF fluorescence using a confocal microscope; scale bars: 10 μm (A). Fluorescence intensity was quantified from more than 100 cells in each replicate by using Image-J and expressed as a fraction of the control (untreated INVc cells) (B). Data represent means ± S.D. from three measurements. Statistical analysis was carried out in SigmaPlot 11.0 by One-Way ANOVA with DMRT. (*) marks significant differences with $p < 0.05$ relative to the likewise treated wild-type.

response to H_2O_2 treatment. As described earlier, *SOD1*, *GPX2* and *TSA2* [40,55] were up-regulated in H_2O_2-treated ADYc cells. *SOD2* was hardly regulated. Upon treatment, BjAnn3 overexpression resulted in transcriptional activation of *SOD1*, *SOD2*, *GPX2* and *TSA2* in INV-ANNw cells, while only *SOD1* and *SOD2* in ADY-ANNw cells, when compared with their respective wild-types. *GPX2* showed no difference, while *TSA2* got down-regulated upon treatment in ADY-ANNw compared to ADYc cells. Overexpression of BjAnn3 affected antioxidant expression. The compensatory activation of these antioxidants for *TSA1* deficiency are in order of *SOD2* < *SOD1* < *GPX2* < *TSA2* in ADYc compared to INVc cells. This order exactly matched the progressive decrease in transcript level of *SOD2* < *SOD1* < *GPX2* < *TSA2* in ADY-ANNw cells compared to ADYc cells. The results from Fig. 6 show that, BjAnn3 interferes with *SOD1*, *SOD2*, *GPX2* and *TSA2* expression, which in turn may help to maintain cellular redox homeostasis. A direct regulatory effect of BjAnn3 in antioxidant expression is unlikely, since annexins are not reported to function as transcription factors (TFs). Probably, BjAnn3 indirectly influences transcript accumulation by modulation of cellular redox homeostasis followed by regulation of redox-regulated TFs. On one hand, BjAnn3 positively regulates these antioxidants upon treatment. But on the other hand, BjAnn3 appears to play a dual role which may either be antagonistic or synergistic depending on the state of the cell.

This report characterizes the effects of heterologous expression of a plant annexin in *S. cerevisiae*. *S. cerevisiae* lacks recognizable annexin-like sequences [56], however, single copies are found in certain yeast species [31]. Annexins are well known membrane

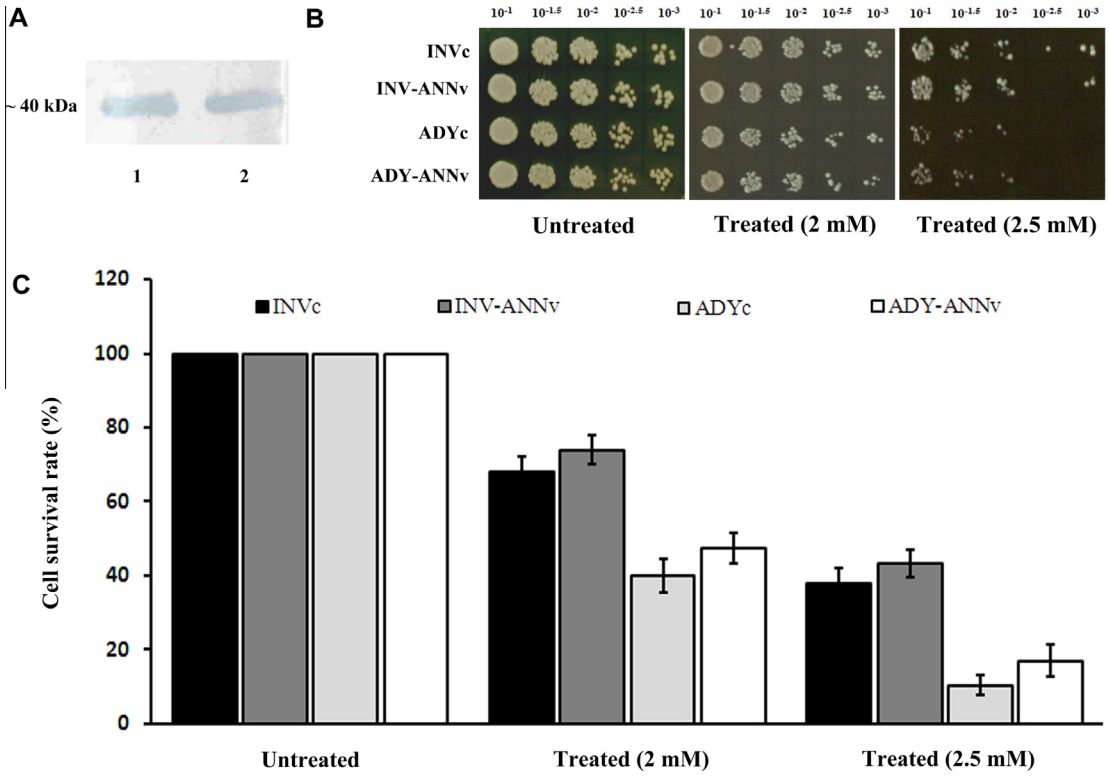

Fig. 5. Recombinant expression of BjAnn3$_{C114S/C242S}$ and its functional effect on the restoration of cell viability during H_2O_2-mediated oxidative stress. (A) Confirmation of BjAnn3$_{C114S/C242S}$ expression in *lane1*, INV-ANNv and *2*, ADY-ANNv cells. Sensitivity of yeast strains INVc, INV-ANNv, ADYc and ADY-ANNv to H_2O_2 was analyzed by spotting (B) and fluctuation assay with cell survival rate in percent of untreated cells (C). Data represent means ± S.D. from three measurements. Statistical analysis was carried out in SigmaPlot 11.0 by One-Way ANOVA with DMRT. (∗) marks significant differences with $p < 0.05$ relative to the likewise treated wild-type.

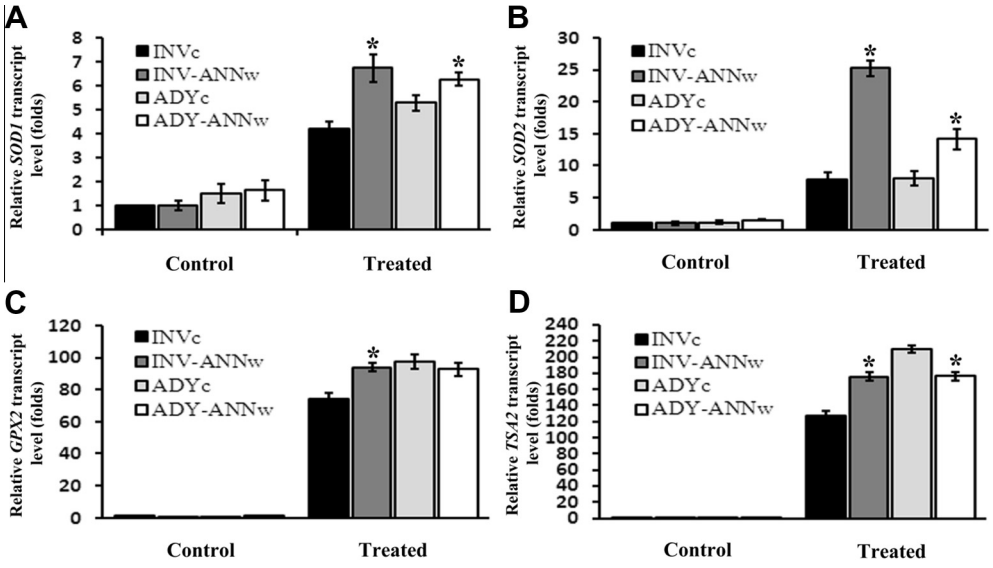

Fig. 6. qRT-PCR analysis of mRNA transcripts of some antioxidant enzymes. All strains showed BjAnn3-mediated regulation upon treatment with 2.5 mM H_2O_2. *SOD1* (A), *SOD2* (B), *GPX2* (C) and *TSA2* (D) transcripts were quantified as described above. *ACT1* was used as reference gene. Data represent means ± S.D. from three measurements. Statistical analysis was carried out in SigmaPlot 11.0 by One-Way ANOVA with DMRT. (∗) marks significant differences with $p < 0.05$ relative to the likewise treated wild-type.

binding proteins [1–3]. They have been studied for their function in cellular-protection, membrane stabilization and ROS detoxification in bacteria, plants and mammalian cell lines [4,10,12,19–23,27]. Here it is shown that, BjAnn3 protects yeast cells from oxidative stress. Two scenarios are possible: (i) BjAnn3 could either directly detoxify ROS or (ii) positively modulates the endogenous antioxidant system and thereby affects ROS accumulation. Expression of BjAnn3 maintained the permeability barrier, which could result either from membrane stabilization by binding [49] or from ROS detoxification in a free or membrane-bound state [3]. Again, ROS detoxification may be due to peroxidase activity of BjAnn3 or due to an interaction with native defense system within the cell.

The methionine residue of S_3 cluster often varies as in BjAnn3, but the two cysteine residues remained conserved [12]. The absence of both heme-binding histidine residue and S_3 cluster in BjAnn3 might suggest that, the conserved cysteine residues are involved in ROS detoxification. This hypothesis is proved from the fact that, BjAnn3 with mutated cysteine residues was not able to compensate the loss of TSA1 function significantly. Annexins are also predicted to function as heme-free glutathione peroxidases, a subgroup of peroxiredoxins, that using conserved cysteines reduce hydroperoxides which act as electron acceptor [22,57,58]. Such a thiol peroxidase activity might be the reason why BjAnn3 complements TSA1-deficient yeast. Our results indicate that, BjAnn3 interferes with other antioxidant genes for ROS modulation. Their evolutionary significance is well concluded form our results, based on their role in transcriptional activation of antioxidant genes and their cross talk with the defense system across kingdom, enabling a cooperative cellular-protection. Despite partial compensation of TSA1 by BjAnn3 in cell-viability tests, the over-complementation in ROS-related features suggests the existence of both redundant (e.g. ROS detoxification) and distinct features (e.g. membrane protection versus proximity-based redox regulator) of both proteins.

Acknowledgements

PBK acknowledges the grant in the form of a research project from the University Grants Commission, India. Facilities used from School of Life Sciences (under DST-FIST and DBT-CREBB), Central Instruments Laboratory and Centre for Nanotechnology at University of Hyderabad, India, are acknowledged. AD gratefully acknowledges UoH-DBT-CREBB, India, and DAAD, Germany, for research fellowships and travel grants. KJD acknowledges support by the German Science Foundation (DFG, Di 346). We thankfully acknowledge Mr. Srikant Prasad Verma, DOEACC society, Kolkata, India, for his contribution of Supplemental Fig. 2. We thank Ms. M. Nalini for her technical expertise in confocal microscopy.

Appendix A. Supplementary data

Supplementary data associated with this article can be found, in the online version, at http://dx.doi.org/10.1016/j.febslet.2014.01.006.

References

[1] Dabitz, N., Hu, N.-J., Yusof, A.M., Tranter, N., Winter, A., Daley, M., Zschörnig, O., Brisson, A. and Hofmann, A. (2005) Structural determinants for plant annexin–membrane interactions. Biochemistry 44, 16292–16300.
[2] Mortimer, J.C., Laohavisit, A., Macpherson, N., Webb, A., Brownlee, C., Battey, N.H. and Davies, J.M. (2008) Annexins: multifunctional components of growth and adaptation. J. Exp. Bot. 59, 533–544.
[3] Laohavisit, A. and Davies, J.M. (2011) Annexins. New Phytol. 189, 40–53.
[4] Gidrol, X., Sabelli, P.A., Fern, Y.S. and Kush, A.K. (1996) Annexin-like protein from *Arabidopsis thaliana* rescues delta oxyR mutant of *Escherichia coli* from H_2O_2 stress. Proc. Natl. Acad. Sci. 93, 11268–11273.
[5] Kovács, I., Ayaydin, F., Oberschall, A., Ipacs, I., Bottka, S., Pongor, S., Dudits, D. and Tóth, E.C. (1998) Immunolocalization of a novel annexin-like protein encoded by a stress and abscisic acid responsive gene in alfalfa. Plant J. 15, 185–197.
[6] Apel, K. and Hirt, H. (2004) Reactive oxygen species: metabolism, oxidative stress, and signal transduction. Annu. Rev. Plant Biol. 55, 373–399.
[7] Lee, S., Lee, E.J., Yang, E.J., Lee, J.E., Park, A.R., Song, W.H. and Park, O.K. (2004) Proteomic identification of annexins, calcium-dependent membrane binding proteins that mediate osmotic stress and abscisic acid signal transduction in Arabidopsis. Plant Cell 16, 1378–1391.
[8] Clark, G.B., Lee, D., Dauwalder, M. and Roux, S.J. (2005) Immunolocalization and histochemical evidence for the association of two different Arabidopsis annexins with secretion during early seedling growth and development. Planta 220, 621–631.
[9] Cantero, A., Barthakur, S., Bushart, T.J., Chou, S., Morgan, R.O., Fernandez, M.P., Clark, G.B. and Roux, S.J. (2006) Expression profiling of the Arabidopsis annexin gene family during germination, de-etiolation and abiotic stress. Plant Physiol. Biochem. 44, 13–24.
[10] Jami, S.K., Clark, G.B., Turlapati, S.A., Handley, C., Roux, S.J. and Kirti, P.B. (2008) Ectopic expression of an annexin from *Brassica juncea* confers tolerance to abiotic and biotic stress treatments in transgenic tobacco. Plant Physiol. Biochem. 46, 1019–1030.
[11] Jami, S.K., Dalal, A., Divya, K. and Kirti, P.B. (2009) Molecular cloning and characterization of five annexin genes from Indian mustard (*Brassica juncea* L. Czern and Coss). Plant Physiol. Biochem. 47, 977–990.
[12] Konopka-Postupolska, D., Clark, G., Goch, G., Debski, J., Floras, K., Cantero, A., Fijolek, B., Roux, S. and Hennig, J. (2009) The role of annexin 1 in drought stress in Arabidopsis. Plant Physiol. 150, 1394–1410.
[13] Zhang, Y., Wang, Q., Zhang, X., Liu, X., Wang, P. and Hou, Y. (2011) Cloning and characterization of an annexin gene from *Cynanchum komarovii* that enhances tolerance to drought and *Fusarium oxysporum* in transgenic cotton. J. Plant Biol. 54, 303–313.
[14] Chu, P., Chen, H., Zhou, Y., Li, Y., Ding, Y., Jiang, L., Tsang, E.W., Wu, K. and Huang, S. (2012) Proteomic and functional analyses of *Nelumbo nucifera* annexins involved in seed thermotolerance and germination vigor. Planta 235, 1271–1288.
[15] Jami, S.K., Clark, G.B., Ayele, B.T., Roux, S.J. and Kirti, P.B. (2012) Identification and characterization of annexin gene family in rice. Plant Cell Rep. 31, 813–825.
[16] Lu, Y., Ouyang, B., Zhang, J., Wang, T., Lu, C., Han, Q., Zhao, S., Ye, Z. and Li, H. (2012) Genomic organization, phylogenetic comparison and expression profiles of annexin gene family in tomato (*Solanum lycopersicum*). Gene 499, 14–24.
[17] Feng, Y.M., Wei, X.K., Liao, W.X., Huang, L.H., Zhang, H., Liang, S.C. and Peng, H. (2013) Molecular analysis of the annexin gene family in soybean. Biol. Plant. 57, 655–662.
[18] Zhou, M.-L., Yang, X.B., Zhang, Q., Zhou, M., Zhao, E.Z., Tang, Y.X., Zhu, X.M., Shao, J.R. and Wu, Y.M. (2013) Induction of annexin by heavy metals and jasmonic acid in *Zea mays*. Funct. Integr. Genomics 13, 241–251.
[19] Jänicke, R.U., Porter, A.G. and Kush, A. (1998) A novel *Arabidopsis thaliana* protein protects tumor cells from tumor necrosis factor-induced apoptosis. Biochim. Biophys. Acta, Mol. Cell. Res. 1402, 70–78.
[20] Kush, A. and Sabapathy, K. (2001) Oxy5, a novel protein from *Arabidopsis thaliana*, protects mammalian cells from oxidative stress. Int. J. Biochem. Cell Biol. 33, 591–602.
[21] Gorecka, K.M., Konopka-Postupolska, D., Hennig, J., Buchet, R. and Pikula, S. (2005) Peroxidase activity of annexin 1 from *Arabidopsis thaliana*. Biochem. Biophys. Res. Commun. 336, 868–875.
[22] Laohavisit, A., Mortimer, J.C., Demidchik, V., Coxon, K.M., Stancombe, M.A., Macpherson, N., Brownlee, C., Hofmann, A., Webb, A.A., Miedema, H., Battey, N.H. and Davies, J.M. (2009) *Zea mays* annexins modulate cytosolic free Ca^{2+} and generate a Ca^{2+}-permeable conductance. Plant Cell 21, 479–493.
[23] Zhou, L., Duan, J., Wang, X.M., Zhang, H.M., Duan, M.X. and Liu, J.Y. (2011) Characterization of a novel annexin gene from cotton (*Gossypium hirsutum* cv CRI 35) and antioxidative role of its recombinant protein. J. Integr. Plant Biol. 53, 347–357.
[24] Clark, G.B., Sessions, A., Eastburn, D.J. and Roux, S.J. (2001) Differential expression of members of the annexin multigene family in Arabidopsis. Plant Physiol. 126, 1072–1084.
[25] Hofmann, A., Delmer, D.P. and Wlodawer, A. (2003) The crystal structure of annexin Gh1 from *Gossypium hirsutum* reveals an unusual S_3 cluster. Eur. J. Biochem. 270, 2557–2564.
[26] Hofmann, A. (2004) Annexins in the plant kingdom: perspectives and potentials. Annexins 1, 51–61.
[27] Konopka-Postupolska, D., Clark, G. and Hofmann, A. (2011) Structure, function and membrane interactions of plant annexins: an update. Plant Sci. 181, 230–241.
[28] Larkin, M.A., Blackshields, G., Brown, N.P., Chenna, R., McGettigan, P.A., McWilliam, H., Valentin, F., Wallace, I.M., Wilm, A., Lopez, R., Thompson, J.D., Gibson, T.J. and Higgins, D.G. (2007) Clustal W and Clustal X version 2.0. Bioinformatics 23, 2947–2948.
[29] Clamp, M., Cuff, J., Searle, S.M. and Barton, G.J. (2004) The Jalview Java alignment editor. Bioinformatics 20, 426–427.
[30] Guttmann, R.P. (2010) Redox regulation of cysteine-dependent enzymes. J. Anim. Sci. 88, 1297–1306.
[31] Clark, G.B., Morgan, R.O., Fernandez, M.P. and Roux, S.J. (2012) Evolutionary adaptation of plant annexins has diversified their molecular structures, interactions and functional roles. New Phytol. 196, 695–712.
[32] Morgan, R.O., Jenkins, N.A., Gilbert, D.J., Copeland, N.G., Balsara, B.R., Testa, J.R. and Fernandez, M.P. (1999) Novel human and mouse annexin A10 are linked to the genome duplications during early chordate evolution. Genomics 60, 40–49.
[33] Bordoli, L., Kiefer, F., Arnold, K., Benkert, P., Battey, J. and Schwede, T. (2008) Protein structure homology modeling using SWISS-MODEL workspace. Nat. Protoc. 4, 1–13.
[34] Harju, S., Fedosyuk, H. and Peterson, K.R. (2004) Rapid isolation of yeast genomic DNA: Bust n'Grab. BMC Biotechnol. 4, 8.
[35] Sambrook, J., Fritsch, E.F. and Maniatis, T. (1989) Molecular Cloning: A Laboratory Manual, second ed, Cold Spring Harbor Laboratory Press.
[36] Montemartini, M., Kalisz, H.M., Hecht, H.J., Steinert, P. and Flohé, L. (1999) Activation of active-site cysteine residues in the peroxiredoxin-type tryparedoxin peroxidase of *Crithidia fasciculata*. Eur. J. Biochem. 264, 516–524.
[37] Pabla, R., Pawar, V., Zhang, H. and Siede, W. (2006) Characterization of checkpoint responses to DNA damage in *Saccharomyces cerevisiae*: basic protocols. Methods Enzymol. 409, 101–117.

[38] Laskar, S., Bhattacharyya, M.K., Shankar, R. and Bhattacharyya, S. (2011) *HSP90* controls *SIR2* mediated gene silencing. PLoS ONE 6, e23406.
[39] Agrimi, G., Brambilla, L., Frascotti, G., Pisano, I., Porro, D., Vai, M. and Palmieri, L. (2011) Deletion or overexpression of mitochondrial NAD^+ carriers in *Saccharomyces cerevisiae* alters cellular NAD and ATP contents and affects mitochondrial metabolism and the rate of glycolysis. Appl. Environ. Microbiol. 77, 2239–2246.
[40] Wong, C.-M., Zhou, Y., Ng, R.W.M., Kung, H.-fu. and Jin, D.-Y. (2002) Cooperation of yeast peroxiredoxins Tsa1p and Tsa2p in the cellular defense against oxidative and nitrosative stress. J. Biol. Chem. 277, 5385–5394.
[41] Li, B.Q. and Tian, S.P. (2006) Effects of trehalose on stress tolerance and biocontrol efficacy of *Cryptococcus laurentii*. J. Appl. Microbiol. 100, 854–861.
[42] Schmitt, M.E., Brown, T.A. and Trumpower, B.L. (1990) A rapid and simple method for preparation of RNA from *Saccharomyces cerevisiae*. Nucleic Acids Res. 18, 3091–3092.
[43] Morano, K.A., Grant, C.M. and Moye-Rowley, W.S. (2012) The response to heat shock and oxidative stress in *Saccharomyces cerevisiae*. Genetics 190, 1157–1195.
[44] Demasi, A.P.D., Pereira, G.A.G. and Netto, L.E.S. (2001) Cytosolic thioredoxin peroxidase I is essential for the antioxidant defense of yeast with dysfunctional mitochondria. FEBS Lett. 509, 430–434.
[45] Garrido, E.O. and Grant, C.M. (2002) Role of thioredoxins in the response of *Saccharomyces cerevisiae* to oxidative stress induced by hydroperoxides. Mol. Microbiol. 43, 993–1003.
[46] Park, S.G., Cha, M.-K., Jeong, W. and Kim, I.-H. (2000) Distinct physiological functions of thiol peroxidase isoenzymes in *Saccharomyces cerevisiae*. J. Biol. Chem. 275, 5723–5732.
[47] Megli, F.M. and Sabatini, K. (2003) EPR studies of phospholipid bilayers after lipoperoxidation: 1. Inner molecular order and fluidity gradient. Chem. Phys. Lipids 125, 161–172.
[48] Megli, F.M., Russo, L. and Sabatini, K. (2005) Oxidized phospholipids induce phase separation in lipid vesicles. FEBS Lett. 579, 4577–4584.
[49] Creutz, C.E., Hira, J.K., Gee, V.E. and Eaton, J.M. (2012) Protection of the membrane permeability barrier by annexins. Biochemistry 51, 9966–9983.
[50] Divya, K., Jami, S.K. and Kirti, P.B. (2010) Constitutive expression of mustard annexin, *AnnBj1* enhances abiotic stress tolerance and fiber quality in cotton under stress. Plant Mol. Biol. 73, 293–308.
[51] Jami, S.K., Hill, R.D. and Kirti, P.B. (2010) Transcriptional regulation of annexins in Indian mustard, *Brassica juncea* and detoxification of ROS in transgenic tobacco plants constitutively expressing *AnnBj1*. Plant Signal. Behav. 5, 618–621.
[52] Lindermayr, C., Saalbach, G. and Durner, J. (2005) Proteomic identification of S-nitrosylated proteins in Arabidopsis. Plant Physiol. 137, 921–930.
[53] Liang, H.P., Brophy, T.M. and Hogg, P.J. (2011) Redox properties of the tissue factor Cys186–Cys209 disulfide bond. Biochem. J. 437, 455–460.
[54] Huh, S.M., Noh, E.K., Kim, H.G., Jeon, B.W., Bae, K., Hu, H.C., Kwak, J.M. and Park, O.K. (2010) Arabidopsis annexins AnnAt1 and AnnAt4 interact with each other and regulate drought and salt stress responses. Plant Cell Physiol. 51, 1499–1514.
[55] Demasi, A.P.D., Pereira, G.A.G. and Netto, L.E.S. (2006) Yeast oxidative stress response. Influences of cytosolic thioredoxin peroxidase I and of the mitochondrial functional state. FEBS J. 273, 805–816.
[56] Gerke, V. and Moss, S.E. (2002) Annexins: from structure to function. Physiol. Rev. 82, 331–371.
[57] Rouhier, N. and Jacquot, J.-P. (2005) The plant multigenic family of thiol peroxidases. Free Radical Biol. Med. 38, 1413–1421.
[58] Dietz, K.-J. (2011) Peroxiredoxins in plants and cyanobacteria. Antioxid. Redox Signal. 15, 1129–1159.